

Published in final edited form as:

*Nat Genet.* 2014 September ; 46(9): 1028–1033. doi:10.1038/ng.3070.

## Jagunal-homolog 1 is a critical regulator of neutrophil function in fungal host defense

Gerald Wirnsberger<sup>1</sup>, Florian Zwolanek<sup>2</sup>, Johannes Stadlmann<sup>1,3</sup>, Luigi Tortola<sup>1</sup>, Shang Wan Liu<sup>1</sup>, Thomas Perlot<sup>1</sup>, Päivi Järvinen<sup>4</sup>, Gerhard Dürnberger<sup>1,3</sup>, Ivona Koziaradzki<sup>1</sup>, Renu Sarao<sup>1</sup>, Alba De Martino<sup>5</sup>, Kaan Boztug<sup>6,7</sup>, Karl Mechtler<sup>1,3</sup>, Karl Kuchler<sup>2</sup>, Christoph Klein<sup>4</sup>, Ulrich Elling<sup>1</sup>, and Josef M. Penninger<sup>1</sup>

<sup>1</sup>IMBA, Institute of Molecular Biotechnology of the Austrian Academy of Sciences, 1030 Vienna, Austria

<sup>2</sup>Medical University of Vienna, Max F. Perutz Laboratories, Department of Medical Biochemistry, 1030 Vienna, Austria

<sup>3</sup>IMP, Institute for Molecular Pathology, 1030, Vienna, Austria

<sup>4</sup>Department of Pediatrics, Dr. Von Hauner Children's Hospital, Ludwig-Maximilians University, Munich, Germany

<sup>5</sup>CSF, Campus Science Support Facility, 1030 Vienna, Austria

<sup>6</sup>CeMM Research Center for Molecular Medicine of the Austrian Academy of Sciences, Vienna, Austria

<sup>7</sup>Department of Pediatrics and Adolescent Medicine, Medical University of Vienna, Austria

### Summary

Neutrophils are key innate immune effector cells essential to fight bacterial and fungal pathogens. Here we report that mice carrying a hematopoietic lineage-specific deletion of Jagunal homolog 1 (*Jagn1*) cannot mount an efficient neutrophil-dependent immune response to the human fungal pathogen *Candida albicans*. Global glyco-biome analysis revealed marked alterations in the glycosylation of proteins involved in cell adhesion and cytotoxicity of *Jagn1*-deficient neutrophils. Functional analysis confirmed marked defects in neutrophil migration in response to *Candida*

---

Correspondence and requests for materials should be addressed to Josef M. Penninger. IMBA, Dr. Bohr Gasse 3, A-1030 Vienna. josef.penninger@imba.oeaw.ac.at.

#### Data codes

All mass spectrometry glycoproteomics data have been deposited to the ProteomeXchange Consortium (<http://proteomecentral.proteomexchange.org>) via the PRIDE partner repository<sup>32</sup> with the dataset identifiers PXD001008 and PXD001009.

#### Author Contributions

Immune phenotyping and flow cytometric analyses were done by G.W. and L.T.. Neutrophil characterization by flow cytometry including cytokine signaling analysis was done by G.W.. U.E. created *Jagn1* conditional mice and the anti-*Jagn1* specific antibody. *Jagn1* full body knock-out mice were made by K.B., F.Z. and K.K. did infection experiments with *Candida albicans*. J.S., G.D., and K.M. performed mass spectrometric analysis of the neutrophil glyco-proteome. S.W. helped with immune phenotyping. I.K. did Western blot analysis and chemotaxis assays. T.P. and L.T. performed Ig isotyping. R.S. performed qPCR analysis. A.D. analyzed histology/cytology and electron microscopy data. G.W., C.K. and J.M.P. designed the experiments and G.W. and J.M.P. wrote the manuscript.

#### Competing Financial Interests

The authors declare no competing financial interests.

*albicans* infection, impaired formation of cytotoxic granules, as well as defective MPO-release and killing of *Candida albicans*. GM-CSF treatment protected mutant mice from increased weight loss and accelerated mortality after *Candida albicans* challenge. Importantly, GM-CSF also restored the defective fungicidal activity of bone marrow cells from patients with *JAGN1* mutations. These data directly identify Jagn1/JAGN1 as a novel regulator of neutrophil function in microbial pathogenesis and uncover a potential treatment option for human patients.

---

Neutrophils are a central arm of innate immune responses against a variety of pathogens relevant in human infectious diseases<sup>1,2</sup>. An impairment of either development or function of these cells has severe pathological consequences characterized by recurrent and often chronic infections due to a failure of the immune system to combat and clear pathogens<sup>3</sup>. In our accompanying paper we report that patients suffering from severe congenital neutropenia carry mutations in Jagunal homolog 1 (*JAGN1*). To test whether *Jagn1* is the causal gene responsible for impaired neutrophil function, we generated *Jagn1* mutant mice.

*Jagn1* is an endoplasmatic reticulum (ER)-resident transmembrane protein encoded by the *Jagn1* gene situated on mouse chromosome 6. We first attempted to generate complete *Jagn1* knock-out mice but never obtained viable *Jagn1* null offspring due to lethality around embryonic day 8.5 for yet unknown reasons (not shown). Consequently, we created mice carrying two LoxP sites flanking exon 2, encoding for the major portion of Jagn1 (Supplementary Fig. 1a), and crossed those mice to a vav-iCre transgenic line that drives Cre expression in all hematopoietic cells<sup>4</sup>. To verify deletion of *Jagn1*, genomic DNA was prepared from spleens and mesenteric lymph nodes (mLN) of control mice carrying two *Jagn1* floxed alleles (hereafter termed *Jagn1<sup>fl/fl</sup>*) or two floxed alleles of *Jagn1* plus the vav-iCre transgene to generate hematopoietic specific *Jagn1* knock-out mice (termed *Jagn1<sup>hem</sup>*). Loss of exon 2 was verified by genomic PCR (Supplementary Fig. 1b) and Western blot analysis (Supplementary Fig. 1c). Cre mediated deletion of *Jagn1* exon 2 led to a loss of Jagn1 protein expression in splenic and mLN derived hematopoietic cells. Moreover, while peripheral blood neutrophils isolated from *Jagn1<sup>fl/fl</sup>* mice expressed readily detectable levels of Jagn1, cells isolated from *Jagn1<sup>hem</sup>* littermate mice did not show any Jagn1 staining (Supplementary Fig. 1d). Thus, we have successfully ablated Jagn1 expression in hematopoietic cells.

Although being expressed in all major hematopoietic lineages tested (Supplementary Fig. 1e), *Jagn1* deletion did not cause any gross abnormalities in total cellularity or cellular composition of mLN, spleen, thymus and bone marrow (Supplementary Figures 1f-j and 2a-f). Furthermore, *Jagn1* deficient hematopoietic progenitors did not show any competitive disadvantage to reconstitute major immune cell lineages in mixed bone marrow chimeric mice (Supplementary Figure 2g-i). Thus, blood cell-specific loss of Jagn1 in mice has no obvious effect on the development of all hematopoietic lineages analyzed and that *Jagn1<sup>hem</sup>* mice exhibit normal numbers of neutrophils in bone marrow, secondary lymphoid organs, and blood.

In mice, neutrophils have been found to be essential to combat infections by the human fungal pathogen *Candida albicans*<sup>5–9</sup>. Since humans with *JAGN1* mutations develop infections prototypic of neutrophil defects (see accompanying paper), we tested the ability of

*Jagn1*<sup>hem</sup> mice to mount an immune response against *Candida albicans*. Systemic *Candida albicans* infection caused significantly more pronounced weight loss in mice that lacked *Jagn1* (Fig. 1a). *Jagn1*<sup>hem</sup> mice also succumbed significantly earlier to *Candida albicans* infection than their control littermates (Fig. 1b). In line with increased morbidity and mortality, we observed massively increased fungal burdens in all tested organs of *Jagn1*<sup>hem</sup> mice (Fig. 1c). The increased fungal burden in *Jagn1* deficient mice was accompanied by a switch to hyphal growth, associated with increased *Candida albicans* virulence and tissue destruction<sup>10</sup>, as assessed by periodic acid-Schiff staining (Fig. 1d). Histologically, we observed severe multifocal tubulo-interstitial nephritis, splenitis with expanded white pulp, and diffuse inflammatory infiltrates into the livers and lungs of *Candida albicans* infected *Jagn1*<sup>hem</sup> mice (Fig. 1d, Supplementary Fig. 3). This data shows that *Jagn1*<sup>hem</sup> mice cannot mount an efficient neutrophil-dependent immune response to *Candida albicans*.

To elucidate the potential mechanism of impaired neutrophil activity, we performed mass-spectrometric analysis of purified bone marrow neutrophils to assess both differences in protein expression and/or protein glycosylation. To this end we applied a novel technology, that we developed recently, to both assess the abundance of N-glycosylations and to map them directly to proteins on a proteome wide scale. We detected specific changes in a limited set of N-glycosylations (Supplementary Fig. 4a and Supplementary Table 1). In particular, we observed an up-regulation of tri-antennary Gal-alpha-1,3-Gal terminated N-glycoforms and a reduction of bi-antennary sialic-acid terminated structures in *Jagn1*<sup>hem</sup> neutrophils (Fig. 2a). Our data thus indicate that loss of *Jagn1* alters glycoprotein-processing and/or protein-trafficking within the ER and Golgi compartments.

Intriguingly, nearly all N-glycosylation changes could be mapped to proteins involved in neutrophil effector functions or their migratory capabilities. In particular, we observed alterations in the glycosylation of the cell adhesion and migration molecules CD177, CD11b (integrin alpha-M), and CD18 (integrin beta-2)<sup>11–15</sup> (Fig. 2b). Moreover, we detected marked alterations in the glycosylation of neutrophil collagenase (*Mmp8*), matrix-metalloproteinase-9 (*Mmp9*), lactoferrin (*Ltf*), Lipocalin 2 (*Lcn2*), haptoglobin (*Hp*), and myeloid batenecin (*F1*) (*Ngp*) (Fig. 2c), molecules implicated in tissue remodeling and cytotoxic effector functions of neutrophils<sup>16</sup>. N-glycosylation differences were equally evident in activated peritoneal neutrophils recruited upon local *Candida albicans* challenge (Supplementary Fig. 4b, Supplementary Table 1). Thus, loss of *Jagn1* results in defined N-glycosylation changes of key molecules involved in neutrophil migration and neutrophil cytotoxicity.

We next wanted to assess whether the pathways uncovered by the glycosylation changes are functionally affected in *Jagn1*-deficient neutrophils. We first assessed mobilization and tissue recruitment of neutrophils. Injection of *Candida albicans* into the peritoneal cavity led to a rapid increase in peripheral blood neutrophil levels when compared to untreated controls both in control and *Jagn1*<sup>hem</sup> mice; (Fig. 3a). In striking contrast, recruitment of neutrophils into the peritoneum was significantly reduced in *Jagn1*<sup>hem</sup> mice (Fig. 3b). This impaired innate immune response to intraperitoneal *Candida albicans* infection was also reflected by significantly decreased TNF $\alpha$  levels in both serum and intraperitoneal lavage of *Jagn1*<sup>hem</sup> mice (Fig. 3c). Moreover, *in vitro* migration assays using Boyden chambers revealed a

marked migratory defect of *Jagn1*<sup>hem</sup> neutrophils in response to the chemoattractant  $\alpha$ MLP (Fig. 3d). We also assessed neutrophil organ recruitment 24 hours after systemic infection with *Candida albicans*. We detected markedly decreased recruitment of *Jagn1*<sup>hem</sup> neutrophils into the kidney and lung (Fig. 3e), a finding that correlates with increased pathogen load in these organs (Fig. 1c). Our data thus indicate that *Jagn1* defective neutrophils cannot effectively migrate to the site of infection following peritoneal or systemic *Candida albicans* challenge.

At later stages of systemic infection we did find an accumulation of macrophages and also neutrophils in kidneys of *Jagn1*<sup>hem</sup> mice (Supplementary Fig. 5), suggesting that, besides the initial recruitment defects, *Jagn1*<sup>hem</sup> immune cells must have functional defects in controlling *Candida albicans* infections. To shed light on the mechanism(s), we first tested for the production of reactive oxygen species (ROS) by neutrophils, dendritic cells, and monocytes/macrophages in *Candida albicans* co-cultures. We did not detect any difference in these cell types with respect to their ability to produce ROS (Fig. 3f). Additionally we assessed the ability these cell types to kill *Candida albicans* using an *in vitro* cytotoxicity assay. Importantly, only *Jagn1* deficient neutrophils showed a reduction in their killing potency (Fig 3g). Of note, phagocytosis of *Candida albicans* by *Jagn1* deficient neutrophils was not impaired (Fig. 3h). These data indicate that *Jagn1* deficient neutrophils, but not *Jagn1* mutant macrophages or dendritic cells, exhibit impaired killing of *Candida albicans*.

To clear microbial pathogens, neutrophils apply a diverse arsenal of cytotoxic substances stored in preformed granules<sup>17</sup>. *Jagn1*<sup>hem</sup> blood neutrophils showed a striking reduction in granularity as detected by flow cytometry (Fig. 4a), resulting from a failure to acquire granularity during their differentiation in the bone marrow (Fig. 4b). At least four types of granules and vesicles have been described in human and mouse neutrophils<sup>16,18</sup>. Our glycoproteom data uncovered alterations in glycosylation of proteins characteristic for primary, secondary, and tertiary granules (Fig. 2c). Electron microscopy studies on purified neutrophils directly confirmed reduced numbers of primary and secondary granules (Fig. 4c,d). In line with diminished primary and secondary granules, we detected markedly reduced levels of the primary granule marker MPO and the secondary and tertiary granule markers MMP8 and MMP9 in blood neutrophils (Supplementary Fig. 6a,b). Since MPO has been identified as, among other pathways, an important neutrophil effector molecule for *Candida albicans* clearance<sup>19–21</sup>, we tested whether reduced levels of MPO extended to impaired MPO release. Indeed we observed a significantly decreased ability of *Jagn1*-deficient neutrophils to release MPO when challenged *in vitro* with *Candida albicans* (Supplementary Fig. 6c). This data shows that loss of *Jagn1* in mice severely affects maturation of neutrophil granules, which are pivotal for their effector functions.

The cytokines G-CSF and GM-CSF are central regulators of neutrophil differentiation and function and G-CSF is routinely used to treat neutropenia<sup>22–24</sup>. In human *JAGN1* mutant patients, we observed defective G-CSF signaling *in vitro* and patients' condition did not improve following G-CSF therapy. We therefore assessed G-CSF signaling in mouse *Jagn1*<sup>hem</sup> neutrophils and observed reduced Signal Transducer and Activator of Transcription (STAT) 3 phosphorylation in murine *Jagn1*-deficient neutrophils upon low dose G-CSF stimulation (Supplementary Fig. 6d). Cell surface expression and total levels of

the G-CSF receptor  $\alpha$  chain (G-CSFR $\alpha$ ) were comparable between control and *Jagn1* mutant neutrophils (Supplementary Fig. 6e). In agreement with defective G-CSF signaling *in vitro*, *Jagn1<sup>hem</sup>* neutrophils also showed a striking reduction in STAT3 phosphorylation following *in vivo* *Candida albicans* infections (Supplementary Fig. 6f). In contrast to impaired G-CSF-R signaling, we observed normal STAT5 phosphorylation in response to GM-CSF stimulation (Supplementary Fig. 6g). Cell surface expression of the GM-CSFR  $\alpha$ -chain was slightly elevated in murine *Jagn1<sup>hem</sup>* neutrophils (Supplementary Fig. 6h).

Remarkably, treatment of isolated bone marrow neutrophils with GM-CSF, but not G-CSF, rescued the impaired MPO release of *Jagn1<sup>hem</sup>* neutrophils and restored their ability to kill *Candida albicans* (Fig. 4e,f). To test whether these *in vitro* rescue experiments could be extended to an *in vivo* situation, we treated *Jagn1<sup>fl/fl</sup>* and *Jagn1<sup>hem</sup>* mice with GM-CSF. While GM-CSF treatment did not affect MPO expression levels in *Jagn1<sup>fl/fl</sup>* blood neutrophils, it partly restored its expression in *Jagn1<sup>hem</sup>* neutrophils (Fig 4g). To test for additional beneficial effects we pre-treated *Jagn1<sup>hem</sup>* and control *Jagn1<sup>fl/fl</sup>* mice with GM-CSF and consequently challenged them with a systemic *Candida albicans* infection to assess neutrophil organ recruitment. Treatment of *Jagn1<sup>hem</sup>* mice with GM-CSF led to a complete rescue of the neutrophil recruitment defects at 24h after systemic infection (Fig. 4h). Most importantly, *in vivo* treatment with GM-CSF completely rescued the enhanced weight loss as well as the reduced survival of *Candida albicans* infected *Jagn1<sup>hem</sup>* mice to levels of GM-CSF treated control *Jagn1<sup>fl/fl</sup>* mice (Fig. 4i,j). Thus, GM-CSF treatment rescues anti-fungal cytotoxicity in *Jagn1* deficient neutrophils and protects mutant mice from accelerated mortality after *Candida albicans* challenge.

Since we observed rescue of the mutant mouse phenotype with GM-CSF treatment, we set out to test whether we could translate this finding to human patients. We obtained bone marrow samples from patient 12 and patient 13 (see accompanying manuscript). These patients have a reduced number of granulocytes in their bone marrow as compared to healthy controls (Supplementary Fig. 6i,j). Importantly, bone marrow granulocytes isolated from *JAGNI* mutant patient 12 did respond to GM-CSF treatment as assessed by intracellular staining for phosphorylated STAT5 (Fig. 4k). We next set up an *in vitro* cytotoxicity assay to test the ability of *JAGNI* mutant cells to kill *Candida albicans*. Cells from *JAGNI* mutant patients were defective in their ability to kill *Candida albicans* as compared to healthy donors. Remarkably, GM-CSF treatment restored their *in vitro* cytotoxic activity to levels observed in control cells (Fig. 4l). These data suggest that GM-CSF treatment might represent an efficacious treatment option for *JAGNI* mutant patients.

Our data identify *Jagn1* as a critical novel regulator of neutrophil migration and effector function and mirror results from *JAGNI*-mutant patients. Inactivation of *Jagn1/JAGNI* causes aberrant granule formation, impaired cytotoxicity towards *Candida albicans*, and defective protein glycosylation. Applying a novel mass spectrometry technique allowed us to directly identify these glycosylation changes and map them to the affected proteins on a proteome wide scale. Our data show that *Jagn1* deficiency in neutrophils results in alterations in N-glycosylation of proteins essential for cell adhesion/migration and neutrophil mediated cytotoxicity. Altered N-glycosylation has already been reported to critically impinge on the function of cell surface molecules like integrins<sup>25–27</sup> or anti-

fungal and anti-bacterial proteins<sup>28–30</sup>. Of note, human *JAGN1*- and mouse *Jagn1*-deficient neutrophils exhibit different alterations in glycosylation reflecting fundamental differences in the glycosylation machinery between mice and men<sup>31</sup>.

Whereas human patients exhibit reduced neutrophil numbers, we did not observe neutropenia in our mutant mice; these differences might be due to the genetic background of our mice, residual expression of mutant *JAGN1* in the human carriers, chronic exposure to pathogens, and/or might reflect species-specific differences, which needs to be explored in additional experiments. Notably, in both human *JAGN1* mutant and mouse *Jagn1* knock-out neutrophils, we found defective signaling via the G-CSF receptor whereas signaling via the GM-CSF receptor was apparently normal. *In vivo* treatment with GM-CSF protected *Jagn1* mutant mice from lethality following septic *Candida albicans* infections. Importantly, our findings in mice translated to human patients: *in vitro* GM-CSF treatment completely restored the defective fungicidal function of bone marrow cells from *JAGN1* mutant patients towards *Candida albicans*. Thus, our murine studies have allowed us to uncover a viable treatment option for *JAGN1* mutant patients, which now needs to be tested in clinical trials.

## Methods

### Generation of *Jagn1* deficient mice

To obtain *Jagn1* conditional mice, targeted ES cells were obtained from Eucomm (clone ID HEPD0614\_4\_D07) and injected into day 3.5 blastocysts. After germline transmission, mice were crossed to vav-iCre transgenic mice<sup>4</sup>. Mouse genotypes were determined by PCR analysis (see Supplementary table 2 for primer sequences). Of note, only age- and sex-matched littermates from the same breeding were used for experiments. All mice were bred and maintained in accordance with ethical animal license protocols complying with the current Austrian law.

### Generation of mixed bone marrow chimeric mice

To generate bone marrow chimeric animals 8 week old CD45.1 *Rag1* deficient mice were irradiated (split dose, 2x6 Gy) and reconstituted 18 hours after the second irradiation with the described mixture of donor cells ( $3 \times 10^6$  donor cells per mouse) by intravenous injection. Experiments were carried out 10 weeks after reconstitution.

### Histology

For histological analysis, 2.5µm thick sections of fixed and paraffin embedded tissues were stained with hematoxylin and eosin (H&E), periodic acid-Schiff (counterstained with hematoxylin), or, for immunohistochemistry, with specific antibodies after antigen retrieval (BOND epitope retrieval Kit, Leica). Specimens were scanned using a Mirax slide scanner. See Supplementary Table 2 for the antibodies used in this study. To assess nuclear morphology and MPO content of peripheral blood neutrophils, blood smears were obtained, dried for 5min, fixed with 4% formaldehyde, stained with H&E or an MPO specific antibody and scanned with a Mirax slide scanner. To analyze the distribution of MPO staining intensity, Definiens Tissue Studio software was applied. To train the software algorithm on differentiating neutrophils and distinguish them from other leukocytes, target

objects and non-target objects were manually classified in a representative area of a slide. The definition of target objects was based on morphology and immunostaining. The optimized algorithm was then applied to analyze all slides automatically. To confirm the quality of the analysis, spot tests were performed on slides from both *Jagn1<sup>fl/fl</sup>* and *Jagn1<sup>hem</sup>* samples.

### Neutrophil isolation and differentiation of dendritic cells and monocytes/macrophages

Neutrophils were isolated from tibias and femurs of mice using a Percoll-gradient (GE Healthcare) as previously described<sup>33</sup> or were sorted using a FACSARIA III cell sorter (BD Biosciences) after anti-Ly6G antibody labeling. Purified neutrophils were cultured in RPMI-1640 media (PAA) and recombinant G-CSF (Biolegend) or GM-CSF (eBioscience) were added into the culture media. Dendritic cells or monocytes/macrophages were obtained by differentiation from bone marrow precursor cells as described<sup>34</sup>. Peripheral blood neutrophils were obtained either by sub-mandibular or tail vein bleeding and collected in potassium EDTA tubes (Sarstedt, Germany). Red blood cells were lysed using Ammonium-Chloride-Potassium (ACK) buffer.

### Flow cytometry and hemocytometry

Antibody labeling of leukocytes was carried out in FACS staining buffer (PBS supplemented with 2% EDTA and 2mM EDTA) on ice for 30min after blocking Fc-receptors. See Supplementary Table 2 for a list of antibodies used in this study. Intracellular staining for the Treg marker FoxP3, cytokines, and *Jagn1* was carried out using the Foxp3 staining Kit (Ebioscience) according to manufacturer's instructions. For cytokine detection, splenocytes were activated with PMA/Ionomycin (100ng/ml and 1µg/ml, respectively) for 3 hours in the presence of Brefeldin A (Ebioscience) prior to cell surface marker staining, fixation and intracellular staining. To study STAT3/5 phosphorylation of murine neutrophils, peripheral blood neutrophils were obtained as described above and stimulated for the indicated periods of time with recombinant mouse GM-CSF (Ebioscience) or G-CSF (Biolegend) at the indicated concentrations. To assess STAT5 phosphorylation of human granulocytes, CD34<sup>-</sup> human bone marrow cells were serum starved for 2 hours and subsequently stimulated with recombinant human GM-CSF (50ng/ml; Ebioscience) for 15 minutes. Intracellular staining for phosphorylated STAT3 and phosphorylated STAT5 was carried out using the Phosflow Kit (BD Bioscience) according to the manufacturer's instructions. Cells were recorded on an LSR II flow cytometer (BD Biosciences) and data analyzed using the FlowJo v10.0.6 software (Tree Star). White and red blood cell counts were obtained using a Vet-abc hematology analyzer (Scil).

### Measurements of cytokine production, MPO release, and ROS

Concentrations of TNFα in the peritoneal lavage and serum were analyzed with plate-bound ELISA kits according to manufacturer's instructions (ELISA Ready-SET-Go, eBioscience). MPO was measured using plate-bound ELISA kits according to manufacturer's instructions (HK210 Mouse MPO, Hycult biotech). Production of reactive oxygen species (ROS) in isolated neutrophils, bone marrow derived dendritic cells, and bone marrow derived monocytes/macrophages was measured with an assay using luminol as the probe in real-time over 120 minutes as described<sup>35</sup>.

### **In vivo fungal infections and GM-CSF treatment**

To test for a role of GM-CSF (Ebioscience) in regulating MPO expression levels of blood neutrophils, 8-10 week old mice were injected intra-peritoneally with 0.5µg of recombinant GM-CSF (Ebioscience) daily for 3 days and bled 24 hours after the last treatment to obtain blood neutrophils for cytological analysis. For *in vivo Candida albicans* challenge 8-10 week old male mice were intravenously infected with  $1 \times 10^5$  colony forming units (CFUs) of *Candida albicans* strain SC5314 in PBS/21.5g mouse weight. Prior to infection, fungi were grown in normal YPD media (2% glucose) at 30°C with agitation. Mice were monitored twice daily and loss of body weight was recorded. For survival experiments, mice were monitored for up to 21 days. For GM-CSF rescue experiments, mice were treated with 0.5µg recombinant murine GM-CSF in PBS or PBS alone as vehicle control by intra-peritoneal injection. Treatment was started 24 hours before infection with *Candida albicans* and mice were subsequently treated with GM-CSF every 48 hours. To determine fungal burdens in different organs, mice were sacrificed and spleen, liver, kidneys, and lung removed aseptically at necropsy, rinsed with sterile PBS, weighed, and placed in 1.5 ml sterile tissue lysis buffer (200 mM NaCl, 5 mM EDTA, 10 mM Tris, 10% glycerol, 1× protease inhibitor cocktail (Roche)) on ice. The organs were aseptically homogenized using an Ika T10 basic Ultra-Turrax homogenizer (Ika, Staufen). Serial dilutions of homogenates were plated in triplicate on YPD (1% yeast extract, 1% peptone, 2% dextrose) plates containing ampicillin, tetracycline, and chloramphenicol. Colonies were counted after 48 hours of incubation at 30°C. The fungal burden was calculated as CFU/g of tissue. For neutrophil recruitment experiments, mice were injected intra-peritoneally with  $5 \times 10^6$  CFUs. After 24 hours, peritoneal cells were collected with ice cold, sterile PBS, and total cell numbers and cellular composition of the infiltrates were analyzed by flow cytometry. For organ recruitment experiments mice were infected intravenously with 100 000 CFU/21.5g bodyweight. 24 hours after *Candida albicans* challenge mice were sacrificed, organs digested with liberase according to the manufacturer's instructions (Roche), filtered through a 70µm mesh and an aliquot stained with Abs against Ly6G, CD45, GR-1, and CD11b and recorded using a LSR II flow cytometer (BD Biosciences).

### **Phagocytosis assay**

Phagocytosis of *Candida albicans* was performed as described<sup>34</sup>. Briefly, *Candida albicans* (strain SC5314) were labeled with Alexa Flour 488 (Invitrogen) in 100mM HEPES buffer (pH 7.5). Isolated neutrophils were then co-cultured with labeled *Candida albicans* for 45 minutes at 37°C. Adherent fungal cells were quenched with Trypan blue (Sigma Aldrich) and the rate of phagocytosis was assessed by flow cytometry.

### **Candida albicans killing assay**

For the *in vitro* killing assays, isolated neutrophils, bone marrow derived dendritic cells and bone marrow derived monocytes/macrophages (all cultured in RPMI-1640), or human CD34<sup>+</sup> bone marrow cells (cultured in Dutch modified RPMI-1640) were plated in replicates at a density of  $1 \times 10^5$  cells/well in 96-well plates. Cells were incubated with *Candida albicans* at a multiplicity of infection of 1:500 for 24 hours. After incubation, neutrophils were fixed by addition of paraformaldehyde to a final concentration of 4%. After fixation,

*Candida albicans* were stained with Crystal Violet (Sigma) and killing was assessed by comparing *Candida albicans* colonies in wells with or without neutrophils.

### Chemotaxis assay

Chemotaxis assays were carried out using 5 $\mu$ m Trans-well chambers (Corning Incorporated). Gradient purified neutrophils were added to the upper chamber and the neutrophil chemoattractant *f*MLP (8 $\mu$ M) to the lower chamber. Migrated neutrophils were recovered from the lower chamber after 60min. Cells were then stained for Ly6G and DAPI and numbers of migrated neutrophils quantified with an LSRII flow cytometer equipped with an HTS plate reader (BD Bioscience). To quantify the rate of chemotaxis, *f*MLP attracted neutrophil numbers were normalized to basal cell migration. Experiments were carried out in triplicates.

### Western blotting

Western blotting was carried out using standard protocols. Blots were blocked for 1 hour with 5% bovine serum albumin in 1  $\times$  TBS/0.1% Tween-20, followed by overnight incubation at 4°C with anti-Jagn1 primary antibodies (clone 3643, directed against the N-terminal part of Jagn1, raised in rabbit, affinity purified against KLH coupled peptides ASRAGPRAAGTDGSDGFQHR) diluted in 5% BSA in 1  $\times$  TBS/0.1% Tween-20. Blots were washed three times in TBST for 15 min follow by incubation with HRP-conjugated secondary antibodies (1:2,500; GE Healthcare # NA9340V) for 45 min at room temperature, washed three times in TBST for 15 min and visualized using enhanced chemiluminescence (ECL Plus, Pierce #1896327). Anti-GAPDH mAbs (HRP conjugates; Cell Signaling #3683) were used to control for protein loading.

### Isotyping of serum antibodies

Serum was collected and assayed for serum antibody concentrations and isotypes by using a MILLIPLEX MAP Mouse Immunoglobulin Isotyping Magnetic Bead Panel (Merck Millipore) according to the manufacturer's instructions.

### Electron Microscopy

Cell pellets were mixed at a 1:1 ratio with 20% BSA as filler and transferred into the 100 $\mu$ m cavity of a 3mm aluminum specimen carrier. The carrier was sandwiched with a flat 3mm aluminum carrier and immediately high pressure frozen in an HPF Compact 01 (Engineering Office M. Wohlwend GmbH, Switzerland). Frozen samples were transferred into a Leica EM AFS-2 freeze substitution unit, subsequently. Samples were substituted in a medium of anhydrous acetone containing 1% Osmium Tetroxide and 0.2% uranyl acetate for 48 h at -90°C, heated at a rate of 2°C/h to -54°C, left at -54°C for 8h, heated at a rate of 5°C/h to -24°C, left at -24°C for 15h, heated at a rate of 24°C/h to 0°C, and left at 0°C for 2.5 hours. Specimens were washed 3 times with anhydrous acetone at 4°C and embedded in Agar 100 Resin. 70nm sections (nominal thickness) were post-stained with 2% aqueous uranyl acetate and Reynold's lead citrate and examined with an FEI Morgagni 268D (FEI, Eindhoven, The Netherlands) operated at 80 kV. Digital images were acquired using an 11 megapixel Morada CCD camera (Olympus-SIS).

## Proteomics and glycoproteomics

For sample preparation, FACS-sorted neutrophils were washed 3 times with PBS. The supernatant was removed and the cell pellets were immediately lysed by the addition of freshly prepared 10M Urea in 120mM Triethylammonium bicarbonate buffer (TEAB, Sigma) to a final concentration of 8M Urea in 100mM TEAB and brief ultra-sonication (ultrasonic processor UP100H, Hielscher, Germany). The samples were reduced (final concentration 5mM Tris(2-carboxyethyl)phosphine hydrochloride, 30 min) and alkylated (final concentration 10mM methyl-methanethiosulfonate, 30min). Protein concentrations were measured (BCA Protein Assay Kit, Pierce) and 1 mg protein per sample was digested with 10µg endoproteinase Lys-C (Wako) for 8 hours at 37°C. The samples were further diluted to 4M Urea in 50 mM TEAB and incubated with 10µg modified porcine trypsin (sequencing grade, Promega) for 12 hours at 37°C. After TMT-6plex-labelling (Thermo) performed according to the supplier's instructions, the pH value of the individual samples was adjusted to approximately 2 by the addition of 10% trifluoroacetic acid (TFA). Samples were pooled in equal amounts, desalted using reversed phase solid-phase extraction cartridges (SPE, Sep-Pak C-18, Waters) and completely dried under vacuum.

For glycopeptide enrichment and mass-spectrometry, glycopeptides were enriched using hydrophilic interaction chromatography (HILIC). The samples were taken up in 80% acetonitrile containing 0.1 % TFA, and were subjected to chromatographic separation on a TSKgel Amide-80 column using a linear gradient from 0.1% TFA in 80% acetonitrile to 0.1% TFA in 40% acetonitrile over 35 minutes (Ultimate 3000, Dionex – Thermo Fischer Scientific). The collected fractions were dried in a speed-vac concentrator. The HILIC enriched sample fractions were individually analyzed by reversed-phase nanoLC-ESI-MS/MS using a hybrid quadrupole-orbitrap mass-spectrometer (qExactive, Thermo), employing higher collision-energy dissociation (HCD) for (glyco-)peptide analysis.

All MS/MS data were processed and analyzed using Xcalibur 2.2 (Thermo Scientific) and Proteome Discoverer 1.4 (PD 1.4, Thermo Scientific). Specialized software tools used for the analysis of MS/MS data from glycopeptides were developed and implemented in-house as “Nodes” to the PD 1.4 software-suite (manuscript in preparation). MS/MS spectra were extracted from the raw-file format, converted into peak lists using the generic Spectrum Exporter Node of PD 1.4 (settings: min. precursor mass = 350 Da, max. precursor mass = 10000 Da, minimum peak count = 5, S/N Threshold 1.5), charge-deconvoluted and de-isotoped (“MS2 Spectrum Processor”, in-house implementation of the algorithm described by36, available as PD 1.4 Node at <http://ms.imp.ac.at/>). Glycopeptide-spectra were analyzed for the presence of potential [peptide + HexNAc]<sup>+</sup> fragment-ions (PD 1.4 Node “Kassonade”, developed in-house, manuscript in preparation). For this, the mass of the respective precursor-ion was iteratively reduced by the masses represented in a glycan-structure database (“SugarBeet”, developed in-house), minus 203.0794 amu. For the peak-matching, fragment-ion charge-states ranging from 1 to the original precursor charge-state were taken into account. In cases where a corresponding potential [peptide + HexNAc]<sup>+</sup> fragment-ion was detected (with a fragment mass-tolerance of 25 mmu) the spectrum was duplicated, with the original precursor ion-mass being set to the mass of the potential [peptide + HexNAc]<sup>+</sup> fragment ion.

For peptide and glycopeptide identification, the processed MS/MS data were searched against the Uniprot mouse reference proteome set (uniprot.org, 47435 entries; as concatenated forward and reverse data-base), using MASCOT (Matrix Science Ltd., version 2.2.07). The parameters for all MS/MS search engine were set to trypsin as protease, allowing for maximally one missed cleavage site, a precursor mass tolerance of 10 ppm, a fragment mass tolerance of 25 mmu, the fixed modification of methylthiolated cysteine, the variable modifications of oxidation (methionine), deamidation (asparagine and glutamine) and hexosamine (asparagine, serine and threonine) and TMT-sixplex (N-terminus and lysine). The resulting peptide-spectrum matches were manually filtered (search-engine rank 1, peptide length  $\geq 7$ ) and adjusted to 1% FDR, using the target-decoy approach. All mass spectrometry glycoproteomics data have been deposited to the ProteomeXchange Consortium (<http://proteomecentral.proteomexchange.org>) via the PRIDE partner repository with the dataset identifiers PXD001008 and PXD001009.

### Patient samples

All material from patients and healthy donors was obtained with informed assent/consent in accordance with the Declaration of Helsinki. The study was approved by the institutional review board at Hannover Medical School. CD34<sup>+</sup> and CD34<sup>-</sup> samples were purified from bone marrow samples using a CD34 MicroBead kit and the AutoMACS Separator (Miltenyi Biotec).

### Statistics

All values in the paper are given as means  $\pm$  standard deviation unless stated otherwise. Comparisons between groups were analyzed using Student's *t*-test. For the Kaplan-Meier analysis a log rank test was performed. Weight loss over time was analyzed using a two-way ANOVA. P values  $< 0.05$  were accepted as statistically significant.

### Supplementary Material

Refer to Web version on PubMed Central for supplementary material.

### Acknowledgments

We thank all members of the Penninger laboratory for helpful discussions and technical support. We thank all members of the IMP-IMBA Biooptics service facility for assistance in cell sorting and image quantification. K.M. is supported by the European Community's Seventh Framework Programme PRIME-XS (262067) and MeioSys (222883-2) and from the Austrian Science Fund SFB F3402, P24685-B24 and TRP 308-N15. K.K. was supported by a grant of the Medical University of Vienna, and in part by a grant from the FWF (FWF-P-25333-B08). C.K. is supported by the ERC, an EU ERARE program (NEUTRO-NET), the DFG Gottfried-Wilhelm-Leibniz program, DFG-SFB914 (Migration of Immune Cells) and the DZIF (German Center for Infection Research). J.M.P. is supported by grants from IMBA, the Austrian National Foundation, the Austrian Academy of Sciences, NEUTRO-NET, and an EU ERC Advanced Grant.

### References

1. Borregaard N. Neutrophils, from marrow to microbes. *Immunity*. 2010; 33:657–70. [PubMed: 21094463]
2. Mocsai A. Diverse novel functions of neutrophils in immunity, inflammation, and beyond. *J Exp Med*. 2013; 210:1283–99. [PubMed: 23825232]

3. Klein C. Genetic defects in severe congenital neutropenia: emerging insights into life and death of human neutrophil granulocytes. *Annu Rev Immunol.* 29:399–413.
4. de Boer J, et al. Transgenic mice with hematopoietic and lymphoid specific expression of Cre. *Eur J Immunol.* 2003; 33:314–25. [PubMed: 12548562]
5. Fulurija A, Ashman RB, Papadimitriou JM. Neutrophil depletion increases susceptibility to systemic and vaginal candidiasis in mice, and reveals differences between brain and kidney in mechanisms of host resistance. *Microbiology.* 1996; 142(Pt 12):3487–96. [PubMed: 9004511]
6. Brown GD, et al. Hidden killers: human fungal infections. *Sci Transl Med.* 2012; 4:165rv13.
7. Lionakis MS, Lim JK, Lee CC, Murphy PM. Organ-specific innate immune responses in a mouse model of invasive candidiasis. *J Innate Immun.* 3:180–99.
8. Lionakis MS, Netea MG. Candida and host determinants of susceptibility to invasive candidiasis. *PLoS Pathog.* 2013; 9:e1003079. [PubMed: 23300452]
9. Vonk AG, Netea MG, Kullberg BJ. Phagocytosis and intracellular killing of *Candida albicans* by murine polymorphonuclear neutrophils. *Methods Mol Biol.* 2012; 845:277–87. [PubMed: 22328381]
10. Sudbery PE. Growth of *Candida albicans* hyphae. *Nat Rev Microbiol.* 9:737–48. [PubMed: 21844880]
11. Sachs UJ, et al. The neutrophil-specific antigen CD177 is a counter-receptor for platelet endothelial cell adhesion molecule-1 (CD31). *J Biol Chem.* 2007; 282:23603–12. [PubMed: 17580308]
12. Wang L, et al. Surface receptor CD177/NB1 does not confer a recruitment advantage to neutrophilic granulocytes during human peritonitis. *Eur J Haematol.* 90:436–7. [PubMed: 23461681]
13. Hentzen ER, et al. Sequential binding of CD11a/CD18 and CD11b/CD18 defines neutrophil capture and stable adhesion to intercellular adhesion molecule-1. *Blood.* 2000; 95:911–20. [PubMed: 10648403]
14. Borjesson DL, et al. Roles of neutrophil beta 2 integrins in kinetics of bacteremia, extravasation, and tick acquisition of *Anaplasma phagocytophila* in mice. *Blood.* 2003; 101:3257–64. [PubMed: 12480703]
15. Anderson DC, Springer TA. Leukocyte adhesion deficiency: an inherited defect in the Mac-1, LFA-1, and p150,95 glycoproteins. *Annu Rev Med.* 1987; 38:175–94. [PubMed: 3555290]
16. Borregaard N, Cowland JB. Granules of the human neutrophilic polymorphonuclear leukocyte. *Blood.* 1997; 89:3503–21. [PubMed: 9160655]
17. Borregaard N, Sorensen OE, Theilgaard-Monch K. Neutrophil granules: a library of innate immunity proteins. *Trends Immunol.* 2007; 28:340–5. [PubMed: 17627888]
18. Segal AW. How neutrophils kill microbes. *Annu Rev Immunol.* 2005; 23:197–223. [PubMed: 15771570]
19. Aratani Y, et al. Severe impairment in early host defense against *Candida albicans* in mice deficient in myeloperoxidase. *Infect Immun.* 1999; 67:1828–36. [PubMed: 10085024]
20. Aratani Y, et al. Critical role of myeloperoxidase and nicotinamide adenine dinucleotide phosphate-oxidase in high-burden systemic infection of mice with *Candida albicans*. *J Infect Dis.* 2002; 185:1833–7. [PubMed: 12085336]
21. Homme M, Tateno N, Miura N, Ohno N, Aratani Y. Myeloperoxidase deficiency in mice exacerbates lung inflammation induced by nonviable *Candida albicans*. *Inflamm Res.* 2013; 62:981–90. [PubMed: 23955550]
22. Welte K, Zeidler C, Dale DC. Severe congenital neutropenia. *Semin Hematol.* 2006; 43:189–95. [PubMed: 16822461]
23. Kullberg BJ, Oude Lashof AM, Netea MG. Design of efficacy trials of cytokines in combination with antifungal drugs. *Clin Infect Dis.* 2004; 39(Suppl 4):S218–23. [PubMed: 15546121]
24. Vonk AG, et al. Treatment of intra-abdominal abscesses caused by *Candida albicans* with antifungal agents and recombinant murine granulocyte colony-stimulating factor. *Antimicrob Agents Chemother.* 2003; 47:3688–93. [PubMed: 14638466]
25. Gu J, et al. Potential roles of N-glycosylation in cell adhesion. *Glycoconj J.* 2012; 29:599–607. [PubMed: 22565826]

26. Janik ME, Litynska A, Vereecken P. Cell migration—the role of integrin glycosylation. *Biochim Biophys Acta*. 2010; 1800:545–55. [PubMed: 20332015]
27. Gu J, et al. A mutual regulation between cell-cell adhesion and N-glycosylation: implication of the bisecting GlcNAc for biological functions. *J Proteome Res*. 2009; 8:431–5. [PubMed: 19053837]
28. Barboza M, et al. Glycosylation of human milk lactoferrin exhibits dynamic changes during early lactation enhancing its role in pathogenic bacteria-host interactions. *Mol Cell Proteomics*. 11 M111 015248.
29. van Veen HA, Geerts ME, van Berkel PH, Nuijens JH. The role of N-linked glycosylation in the protection of human and bovine lactoferrin against tryptic proteolysis. *Eur J Biochem*. 2004; 271:678–84. [PubMed: 14764083]
30. Van Antwerpen P, et al. Glycosylation pattern of mature dimeric leukocyte and recombinant monomeric myeloperoxidase: glycosylation is required for optimal enzymatic activity. *J Biol Chem*. 285:16351–9.
31. Antonopoulos A, North SJ, Haslam SM, Dell A. Glycosylation of mouse and human immune cells: insights emerging from N-glycomics analyses. *Biochem Soc Trans*. 2011; 39:1334–40. [PubMed: 21936811]
32. Vizcaino JA, et al. The PRoteomics IDentifications (PRIDE) database and associated tools: status in 2013. *Nucleic Acids Res*. 2013; 41:D1063–9. [PubMed: 23203882]
33. Boxio R, Bossenmeyer-Pourie C, Steinckwich N, Dournon C, Nusse O. Mouse bone marrow contains large numbers of functionally competent neutrophils. *J Leukoc Biol*. 2004; 75:604–11. [PubMed: 14694182]
34. Bourgeois C, Majer O, Frohner I, Kuchler K. In vitro systems for studying the interaction of fungal pathogens with primary cells from the mammalian innate immune system. *Methods Mol Biol*. 2009; 470:125–39. [PubMed: 19089381]
35. Frohner IE, Bourgeois C, Yatsyk K, Majer O, Kuchler K. *Candida albicans* cell surface superoxide dismutases degrade host-derived reactive oxygen species to escape innate immune surveillance. *Mol Microbiol*. 2009; 71:240–52. [PubMed: 19019164]
36. Nielsen ML, Savitski MM, Zubarev RA. Improving protein identification using complementary fragmentation techniques in fourier transform mass spectrometry. *Mol Cell Proteomics*. 2005; 4:835–45. [PubMed: 15772112]

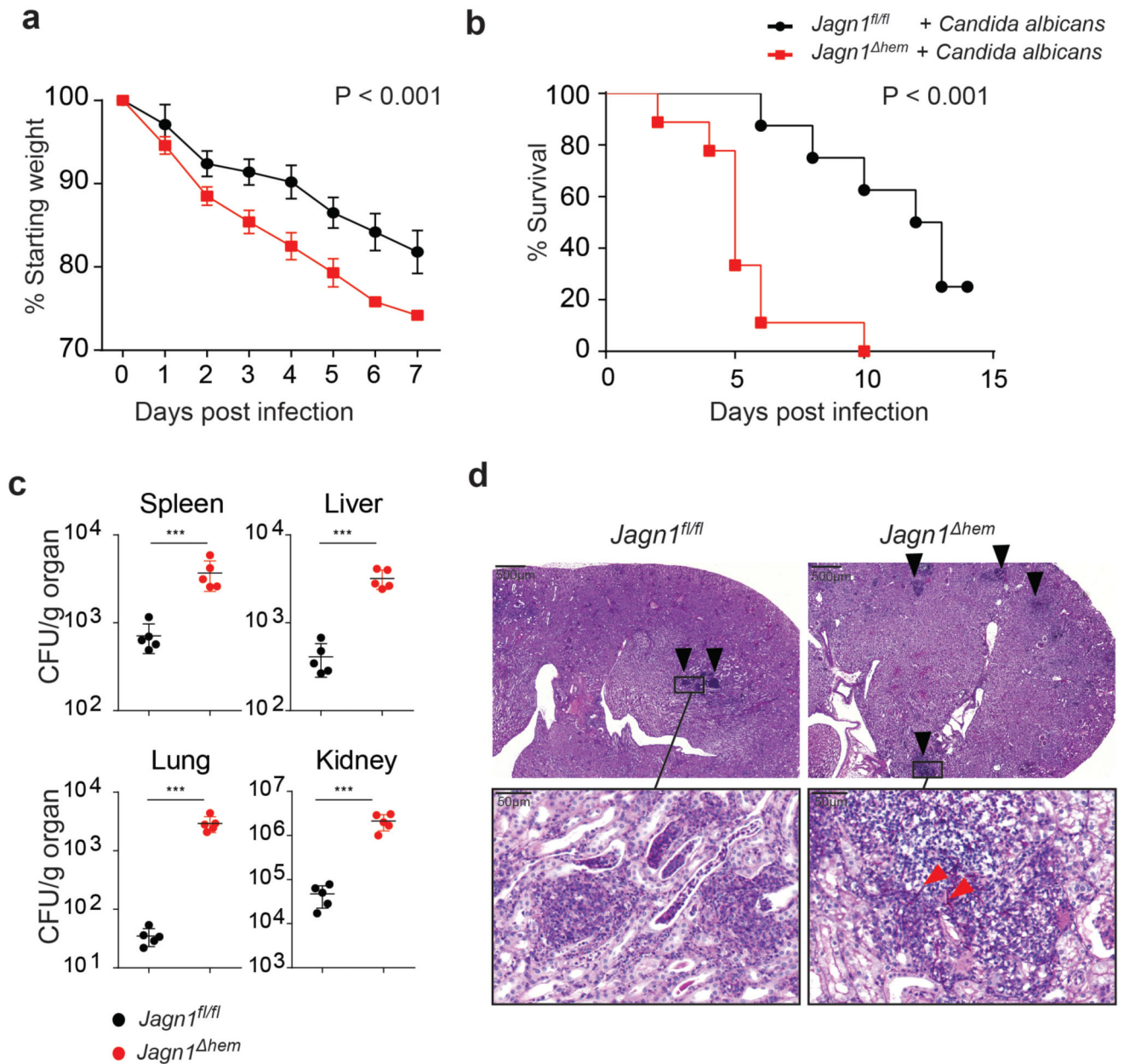


**Figure 1. Hematopoietic deletion of *Jagn1* impairs neutrophil-dependent immune responses against *Candida albicans*.**

(a,b) Control *Jagn1<sup>fl/fl</sup>* and knock-out *Jagn1<sup>hem</sup>* littermate mice were infected intravenously with *Candida albicans* ( $10^5$  CFU/21.5g body weight) and monitored for the indicated time periods. Plots depict (a) weight loss over time after infection as compared to starting weight (p value assessed by two-way ANOVA) or (b) survival over time after infection (p value assessed with log rank test). Data are shown as means  $\pm$  SD.  $n = 8$  for *Jagn1<sup>fl/fl</sup>* and  $n = 9$  for *Jagn1<sup>hem</sup>* mice. (c) *Candida albicans* loads in various organs at day 3 after infection are plotted as colony forming units (CFU) per gram organ weight. Data are shown as means  $\pm$  SD. Each data point represents an individual mouse. \*\*\*  $P < 0.001$ , Student's t-test. (d)

Representative kidney sections from mice 3 days after *Candida albicans* infection, stained with periodic acid-Schiff. Inflammatory infiltrates are indicated by black arrow heads. Boxed areas in the upper panels (50 x magnification) are shown in the lower panels (600 x magnification). Note the presence of *Candida albicans* hyphae in the *Jagn1<sup>hem</sup>* kidney (red arrow heads).

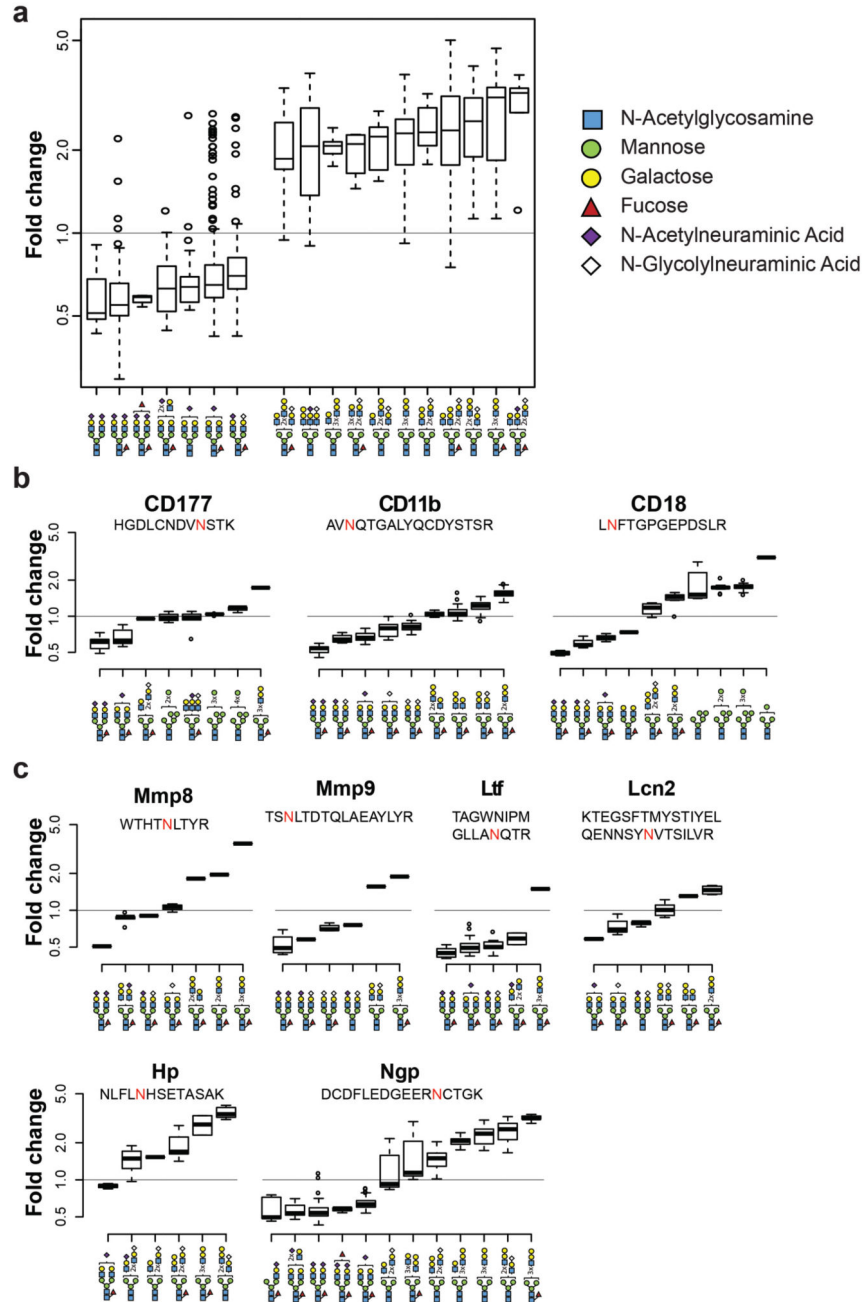


**Figure 2. Loss of *Jagn1* impairs N-glycosylation of neutrophil homing and effector molecules.** (a) Ratios of N-glycan structures in *Jagn1*<sup>hem</sup> versus *Jagn1*<sup>fl/fl</sup> bone marrow neutrophils that are affected by the loss of *Jagn1*. The defined glycan structures are indicated. See Supplementary Fig. 4 for complete glyco-proteomic profiles. (b,c) Schematic depiction of N-glycan structures on (b) a selected set of proteins involved in adhesion and migration of neutrophils and (c) proteins involved in tissue remodeling and cytotoxic effector functions of neutrophils that are affected by the loss of *Jagn1*. Positions of glycosylated asparagines (N) are indicated in red. Shown are the ratios for the indicated glycan structures in *Jagn1*<sup>hem</sup>

versus *Jagn1<sup>fl/fl</sup>* neutrophils. Ratios below 1 indicate downregulation in knock-out neutrophils, ratios above 1 show upregulation in *Jagn1<sup>hem</sup>* knock-out cells. In all panels, data are shown as box-and-whiskers-plots. Horizontal bars indicate the median; boxes span the respective interquartile range; whiskers extend to 1.5 interquartile range; outliers are indicated by circles. n = 3 neutrophils isolated from three different mice for each genotype.

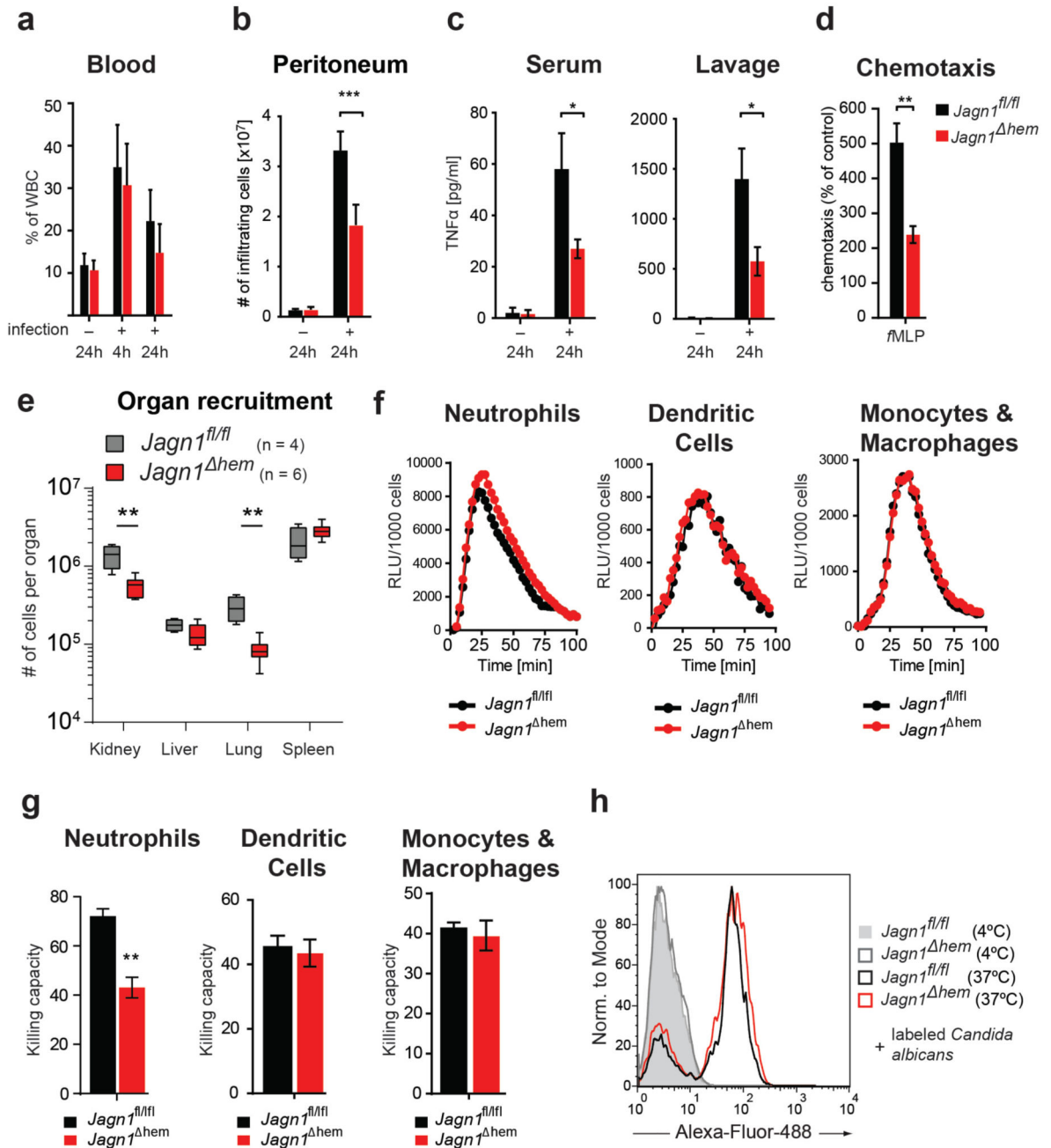


**Figure 3. *Jagn1* deficient neutrophils exhibit impaired migration and killing of *Candida albicans*.**

(a,b) *Jagn1<sup>fl/fl</sup>* and *Jagn1<sup>Δhem</sup>* littermate mice were injected intraperitoneally with  $5 \times 10^6$  CFU of *Candida albicans* or PBS as a control, and (a) mobilization of neutrophils into the blood stream or (b) recruitment into the peritoneum were measured at the indicated time points. Data are shown as means  $\pm$  SD.  $n = 3$  per genotype for blood mobilization and  $n = 6$  per genotype for intraperitoneal recruitment. (c) Serum and intraperitoneal lavage levels of TNF $\alpha$  as assayed by ELISA 24 hours after intraperitoneal infection with *Candida albicans*. Data are shown as mean values  $\pm$  SD.  $n = 3$  per genotype. (d) *f*MPLP induced chemotaxis of

neutrophils. Plot depicts the fMLP induced chemotactic responses of bone marrow neutrophils in a transwell assay. Assays were done in triplicates. Data are shown as mean percentages of chemotaxis as compared to the baseline (set to 100%)  $\pm$  SD. **(e)** Control *Jagn1<sup>fl/fl</sup>* and knock-out *Jagn1<sup>hem</sup>* littermate mice were infected intravenously with *Candida albicans* ( $10^5$  CFU/21.5g body weight) or PBS as a control and neutrophil organ recruitment was assessed 24 hours later. n = 4 for *Jagn1<sup>fl/fl</sup>* and n = 6 for *Jagn1<sup>hem</sup>*. Whiskers extend to minimum and maximum values, respectively. **(f)** Reactive oxygen species (ROS) production by bone marrow neutrophils, bone marrow derived dendritic cells, and bone marrow derived monocytes/macrophages co-cultured with *Candida albicans* and monitored in real time over the indicated time period using the luminol assay. Experiments were performed in triplicates. Values are expressed as relative light units per 1000 cells. **(g)** Killing capacity of *Jagn1<sup>fl/fl</sup>* and *Jagn1<sup>hem</sup>* bone marrow neutrophils, bone marrow derived dendritic cells, and bone marrow derived monocytes/macrophages as assessed by 24 hour co-culture with *Candida albicans*. Assays were performed in sextuplicates. **(h)** Phagocytosis of *Candida albicans*. Neutrophils of the indicated genotypes were isolated from the bone marrow and co-cultured with Alexa Fluor 488 labeled *Candida albicans* at either 4°C (negative control) or at 37°C. After 45 minutes of co-culture, neutrophils were analyzed for *Candida albicans* uptake by flow cytometry. Data are shown as means  $\pm$  SD. \* P < 0.05, \*\* P < 0.01, \*\*\* P < 0.001 as calculated with Student's t-test.

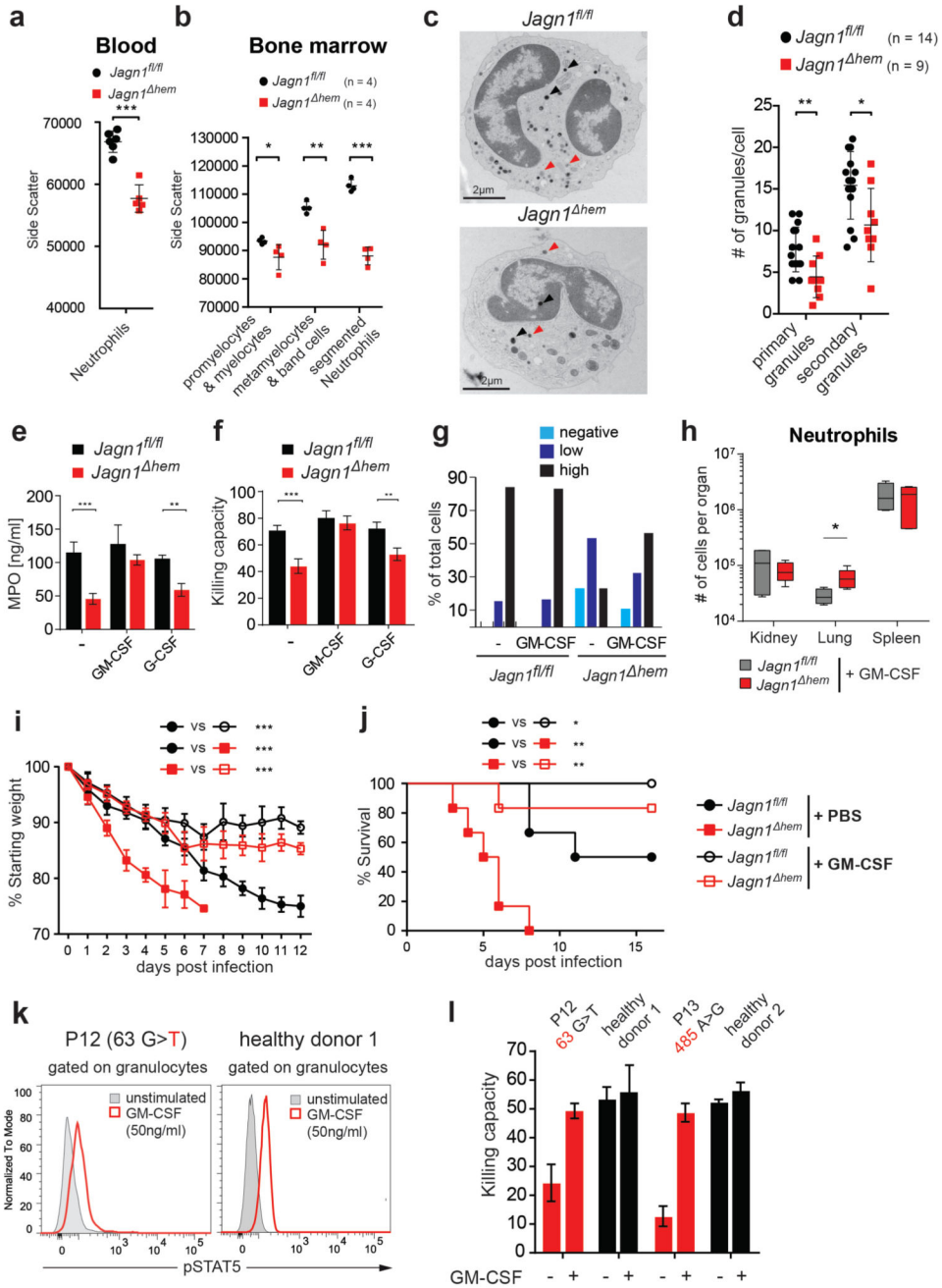


**Figure 4. Jagn1 controls neutrophil granules and anti-fungal cytotoxicity.**

(a,b) Decreased granularity of *Jagn1*-deficient peripheral blood neutrophils (a) and the indicated bone marrow neutrophil precursor populations (b) as detected by flow cytometry. Each data point represents an individual mouse. (c) Representative electron micrographs of segmented neutrophils isolated from the bone marrow of *Jagn1<sup>fl/fl</sup>* and *Jagn1<sup>hem</sup>* mice. 36000x magnifications. Black arrowheads indicate primary, red arrowheads secondary granules. (d) Quantitation of primary and secondary granule numbers of segmented bone marrow *Jagn1<sup>fl/fl</sup>* and *Jagn1<sup>hem</sup>* neutrophils. (e) MPO release from purified bone marrow

neutrophils co-cultured with *Candida albicans* for 24 hours as measured by ELISA in triplicates with or without recombinant murine GM-CSF or recombinant murine G-CSF (100ng/ml each). **(f)** Killing capacity of *Jagn1<sup>fl/fl</sup>* and *Jagn1<sup>hem</sup>* bone marrow neutrophils as assessed by 24 hour co-culture of *Candida albicans* with or without recombinant murine GM-CSF or recombinant murine G-CSF (100ng/ml each). Assays were performed in sextuplicates. **(g)** MPO expression in neutrophils after *in vivo* treatment with GM-CSF. Mice of the indicated genotypes were treated daily with recombinant murine GM-CSF (0.5µg) for 3 days or left untreated. MPO expression in blood neutrophils was assessed subsequently by staining with an MPO specific antibody. Neutrophils were scored based on staining intensity as cells expressing no MPO (negative), low levels of MPO (low), and high levels of MPO (high). Plot depicts the distribution of MPO expression levels in neutrophil populations of the indicated genotype with or without GM-CSF treatment (n = 18/32 for *Jagn1<sup>fl/fl</sup>* untreated/treated and n = 43/37 for *Jagn1<sup>hem</sup>* untreated/treated). **(h)** 24 hours after *in vivo* GM-CSF pre-treatment control *Jagn1<sup>fl/fl</sup>* and knock-out *Jagn1<sup>hem</sup>* littermate mice were infected intravenously with *Candida albicans* (10<sup>5</sup> CFU/21.5g body weight) or PBS and neutrophil recruitment into the indicated organs was assessed 24 hours later. n = 4 for *Jagn1<sup>fl/fl</sup>* and n = 5 for *Jagn1<sup>hem</sup>* mice. Whiskers of Box plots extend to minimum and maximum values, respectively. **(i)** Weight loss over time after infection as compared to starting weight and **(j)** survival after infection of *Jagn1<sup>fl/fl</sup>* and *Jagn1<sup>hem</sup>* mice infected i.v. with *Candida albicans* (10<sup>5</sup> CFU/21.5g body weight). Mice were treated with either PBS or recombinant murine GM-CSF (0.5µg) every 48 hours (starting 1 day before *Candida albicans* infection) and monitored for the indicated time periods. n = 6 mice for each cohort. **(k)** CD34<sup>+</sup> bone marrow cells from the indicated *JAGN1* mutant patient and a healthy donor were stimulated with recombinant human GM-CSF for 15 min and then assayed for phosphorylation of STAT5 (pSTAT5) by intracellular staining. Histogram overlays are shown for cells stimulated with human GM-CSF or left unstimulated. **(l)** Killing capacity of CD34<sup>+</sup> bone marrow cells from the indicated *JAGN1* mutant patients or healthy controls as assessed by 24 hour co-culture with *Candida albicans* with or without recombinant human GM-CSF (50ng/ml). Assays were performed in quadruplicates. In all panels except h, data are shown as mean ± SD. P values were calculated using the Student's t-test with the exception of panel **(i)** (two-way ANOVA over the entire time period) and panel **(j)** (log rank test). \* P < 0.05, \*\* P < 0.01, \*\*\* P < 0.001.